Incorporation of lithium and nitrogen into CVD diamond thin films

M. Zamir Othman [a], Paul W. May [a,*], Neil A. Fox [a], Peter J. Heard [b]

[a] School of Chemistry, University of Bristol, Bristol BS8 1TS, United Kingdom
[b] Interface Analysis Centre, H.H. Wills Physics Laboratory, University of Bristol, Tyndall Avenue, Bristol BS8 1TL, United Kingdom

ARTICLE INFO

ABSTRACT

High concentrations of lithium ($\sim 5 \times 10^{19}$ cm^{-3}) and nitrogen ($\sim 3 \times 10^{20}$ cm^{-3}) have been simultaneously incorporated into single-crystal and microcrystalline diamond films using Li$_3$N and gaseous ammonia as the sources of Li and N, respectively. Using sequential deposition methods, well-defined localised layers of Li:N-doped diamond with a depth spread of less than ± 200 nm have been created within the diamond. The variation in Li:N content and amount of diffusion within the various types of diamond suggests a model whereby these atoms can migrate readily through the grain-boundary network, but do not migrate much within the grains themselves where the diffusion rate is much slower. However, the high electrical resistivity of the doped films, despite the high Li and N concentrations, suggests that much of the Li and N are trapped as electrically inactive species.

1. Introduction

Despite recent developments in doping diamond films with phosphorus, antimony, arsenic and sulfur, the production of n-type semiconducting diamond with useful electronic properties remains elusive [1–11]. Nitrogen is another possible dopant, and nitrogen-doped diamond has been successfully synthesised using hot-filament (HF) chemical vapour deposition (CVD) and microwave plasma CVD (MWCVD) techniques [3,12–17]. However, due to its high activation energy (1.7 eV), nitrogen-doped diamond is an insulator at room temperature, and only becomes semiconducting at high temperatures which makes it impractical for use in most devices.

Recently, lithiated diamond surfaces were suggested as a method to produce low-work-function materials [18–20], and theoretical studies have predicted that interstitial lithium should act as a shallow donor [21]. The energy to excite an electron from the lithium donor level to the conduction band of diamond is calculated to be less than 0.3 eV [22], however this has proved difficult to obtain experimentally, partly due to the low solubility of Li in diamond [23]. Research has been focused on trying to force Li into the diamond lattice by implantation [24–28], diffusion [29,30] and addition of Li species to the gas phase during CVD [31–33]. Although Li was incorporated inside the diamond lattice to values as high as 1×10^{21} cm^{-3} [31], in all cases the Li remained electrically inactive. The proposed explanation for this is the high mobility of Li in diamond at high temperature, which causes diffusion and aggregation of the Li into inactive clusters [29]. To overcome this, it has been suggested [34,35] that Li diffusion can be prevented by simultaneously adding nitrogen together with Li, with the N acting as a trap

to pin down the Li in the diamond lattice and reduce its mobility. In such a system, the electrons from the pinned interstitial Li are transferred through a substitutional N atom directly into the diamond lattice. Thus, it is suggested [34] that if a suitable co-doping process can create defect sites with a 1:1 ratio of Li:N, this could produce n-type semiconducting diamond with a shallow donor level and high electron mobility. More recent theoretical work has suggested that shallow donor states may be also created using LiN$_4$ clusters [36], requiring a 1:4 ratio of Li:N in the diamond lattice. However, no experimental work has yet been reported to test these hypotheses.

In this paper, we present the results of a study to incorporate significant concentrations of both Li and N while growing diamond thin films using a HF–CVD system. The experiments involve both simultaneous co-doping, as well as sequential doping to form layers of differently doped diamond. Secondary ion mass spectrometry (SIMS) depth-profile analysis is presented to show the concentration of both dopants and the thickness of the dopant layers inside the diamond film.

2. Experimental

Two types of substrates were used for the diamond growth, either 1 cm^2 single-crystal Si wafers (100) which were pre-treated by a manual abrasion technique using 1–3 μm diamond particles, or high-pressure high-temperature (HPHT) single-crystal diamond (2.5 × 2.5 mm^2) type 1b (100) (purchased from Element Six, Ltd.). The latter did not require any pre-treatment or seeding, but were cleaned in an acid bath to remove any non-diamond material prior to CVD.

Diamond was deposited in a HF reactor using standard CVD conditions with the distance between the substrate and the tantalum filament fixed at 3 mm. Undoped diamond was deposited using a standard ratio of 0.82% CH$_4$ in H$_2$. The process pressure was set

at 20 Torr while the filament temperature was measured using an optical pyrometer and maintained between 2100 and 2250 K. These conditions fabricated faceted microcrystalline diamond (MCD) at a rate of ~0.5 μm h^{-1}.

Nitrogen-doped diamond was deposited by adding either N_2 or NH_3 to the gas mixture such that the N:C ratios were 0.7 and 0.4, respectively. These values were chosen because from previous experiments [37] it was known that additions of N_2 higher than this begin to significantly increase the growth rate and alter the morphology of the resulting diamond films, which we wished to avoid. The gas-phase concentration of N_2 was deliberately made much higher than that of NH_3 in an attempt to compensate for the difficulty of dissociating the strong N_2 bonds using a HF system [38].

Lithium nitride (Li_3N) was used as a source of Li, which is available commercially as a powder (CERAC, 99.5% purity, <250 μm particle size). Initially, a series of experiments were performed to identify a suitable liquid medium that would support a stable suspension of Li_3N. Water and alcohols were ruled out because they oxidised the Li_3N to LiOH. Various other oxygen-free liquids were tried (heptane, xylene, hexane, cyclohexane, toluene, chloroform) and the general trend was that the stability of the suspension increased with increasing polarity of the liquid, with chloroform being the best of those tested. However, even in chloroform the suspensions only remained stable for 1–2 days. This stability period could be improved to several weeks by the addition to the suspension of a polar polymer, such as polyoxyethylene ether (POE) or polysorbate-20. Our final optimised suspension was prepared by dissolving 5 mg of POE in 5 ml of chloroform, followed by the addition of 85 mg of Li_3N powder. The reddish-black suspension was then sonicated for 1 h in an ultrasonic bath.

To incorporate Li into the diamond film, this Li_3N suspension was drop cast onto the surface of the substrate. For some samples, the suspension was drop cast directly onto the Si substrate. But it was later found that Li diffused easily into the Si, and so to prevent this usually a thin (2–3 μm) layer of N-doped CVD diamond was deposited onto the Si substrate as a diffusion barrier before dropcasting the Li_3N suspension. For a given sample, the same CVD conditions were used for this initial diamond layer as for any subsequent N-doped diamond layers. The amount of suspension used depended on the substrate size: 7–20 μl for the smaller HPHT diamond substrates and ~100–300 μl for the CVD diamond films on the larger Si substrates. For such small area samples and low-viscosity liquids, spin coating to achieve uniform coverage is not practicable, but could easily be implemented if this process were ever to be upscaled to wafer sizes. As a result, there would undoubtedly have been some non-uniformities of coverage and hence variations in doping levels around the periphery of the samples, but, to minimise these, all characterization measurements were performed in the central region of the samples. The suspension was then allowed to dry (which took a few seconds) before the substrate was placed into the HFCVD reactor, whereupon it was heated by the filament (2100 K) in a pure H_2 atmosphere for an hour at a surface temperature of about 800 °C (estimated by 2-colour pyrometer). This served to melt the Li_3N powder and to partially diffuse Li and N into the diamond surface to form a Li/N co-doped layer 100–200 nm thick (estimated by subsequent SIMS measurements). Care had to be taken not to overheat the surface during this period or the molten Li_3N would evaporate and be pumped away.

Finally, this molten layer was encapsulated into the film by depositing on top of it a capping layer of nitrogen-doped diamond using the CVD conditions described above. The thickness of this capping layer varied from a few 100 nm to ~5 μm depending on the growth time. For some experiments the Li_3N deposition and capping layer growth steps were repeated several times in order to build up sequential layers of varying Li/N concentrations within the diamond film.

The film morphology, quality and concentration of dopants were characterised using scanning electron microscopy (SEM), laser Raman spectrometry and SIMS. For SIMS, the Li signal was detected as Li^+

while the nitrogen signal was detected as CN^-. The absolute concentrations of N and Li in the diamond were quantified using exemplar single-crystal diamond samples previously implanted with known concentrations of Li and N for use as SIMS calibration. The minimum detection limit for Li in the instrument was 2.03×10^{17} cm^{-3}. Because CVD diamond may contain hydrogen, it is possible that some of the SIMS signal at mass 26 might be due to a contribution from $C_2H_2^-$ as well as from CN^-. To determine the magnitude of this unwanted contribution, an undoped CVD film was deposited onto an N-doped diamond film, and the relative signal at mass 26 compared for both layers as the SIMS depth profile etched through both layers. The signal for the undoped layer which was wholly from $C_2H_2^-$ determined the lower limit for N detection at 1.15×10^{19} cm^{-3}, while the signal for the N-doped layer was ~50 times higher. Thus, it was relatively easy to distinguish the signal from CN^- from the background due to $C_2H_2^-$. All data and graphs are plotted after subtracting the $C_2H_2^-$ background signal to obtain the concentration of N atoms, with an estimated uncertainty of ~5%.

Another potential problem with using SIMS for depth profiling on non-flat samples is that large variations in the surface roughness might affect the sharpness of any layer boundaries. This problem is machine-dependent: etching/depth-profiling in some SIMS instruments planarises the initial surface morphology making the problem negligible, whereas in some SIMS instruments the height difference of surface features becomes magnified as etching proceeds, severely broadening the layer profiles. To determine if this was a problem in our SIMS, two CVD films were grown with approximately the same thickness (3 μm) but with different morphologies. The first was an MCD film with surface grain size (and hence approximate surface r.m.s. roughness) of ~1 μm as measured by SEM. The second was a smoother nanocrystalline diamond (NCD) film with grain size and surface roughness ~100 nm. Both films were grown onto a Si substrate known to support a native-oxide layer of thickness ~100 nm. SIMS depth profiles were performed on both samples, and the full-width half-maximum of this oxide layer was measured after etching through the overlying diamond film. The two measured values were 98 nm and 103 nm for the MCD and NCD films, respectively, which are the opposite of what might be expected if surface roughness blurred layer boundaries. Therefore, we conclude that in our SIMS system the initial surface morphology is not a problem when measuring the sharpness of layer boundaries, and the reproducibility of the system due to surface roughness, SIMS mixing and other effects is ±10 nm in diamond samples.

Electrical resistance measurements were performed using a two-point probe method. All samples underwent ozone treatment to change
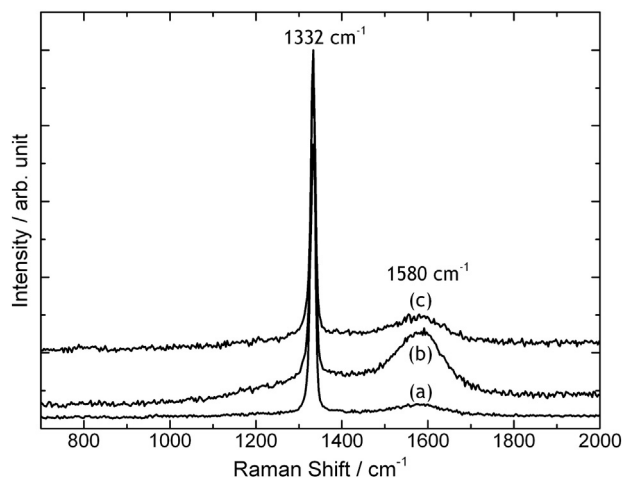

Fig. 1. Laser Raman spectrum (325 nm He–Cd excitation) obtained from different layers of the microcrystalline diamond films grown on Si. (a) Undoped diamond, (b) nitrogen-doped diamond, and (c) Li/N-co-doped diamond.

the hydrogen-terminated surface of the as-grown diamond to an oxygen-terminated surface in order to eliminate any possible surface conductivity [3]. Two 1×1 mm^2 silver contacts were evaporated on top of the diamond film at the diagonal corners of each sample separated by a distance of ~10 mm allowing the bulk electrical resistance to be measured.

3. Results & discussion

3.1. Film characterization

Laser Raman spectra (325 nm excitation) taken from the three types of diamond layer grown on Si substrates are shown in Fig. 1. The Li–N-co-doped diamond layer exhibited a typical Raman spectrum that was very similar to that from undoped CVD diamond films grown with the same CH$_4$ content. The diamond peak at 1332 cm^{-1} and graphitic G-band at ~1580 cm^{-1} are present as expected for microcrystalline films, but no new peaks corresponding to N or Li are observed. Further

Raman spectra using 514 nm excitation (not shown) from the 3 types of diamond gave the same findings.

Fig. 2 shows the morphology of the microcrystalline diamond layers before and after the addition of lithium nitride. The nitrogen-doped diamond exhibited microcrystalline facets (Fig. 2(a,b)), as expected. After addition of Li$_3$N the facets became much rougher (Fig. 2(c,d)), suggesting that new nucleation sites had been created, possibly as a result of localised etching of the surface by Li [39]. The etching and surface modification only occurred on the surface in a layer less than 100 nm in thickness (Fig. 2(e)). Based on the micrographs and Raman spectra in Fig. 1, we suggest that the Li preferentially etches the graphitic carbon at the grain boundaries of the diamond thin film. This might explain the reduction of the graphitic feature at 1580 cm^{-1} in Fig. 1 suggesting the apparent improvement in diamond quality due to the removal of some of the grain-boundary sp^2 carbon.

Further evidence for this theory comes from Fig. 3, which shows the morphology of the nitrogen-doped diamond capping layer grown on top of the Li/N co-doped layer on a HPHT substrate. Fig. 3(a) shows the surface of the single-crystal HPHT diamond substrate before the
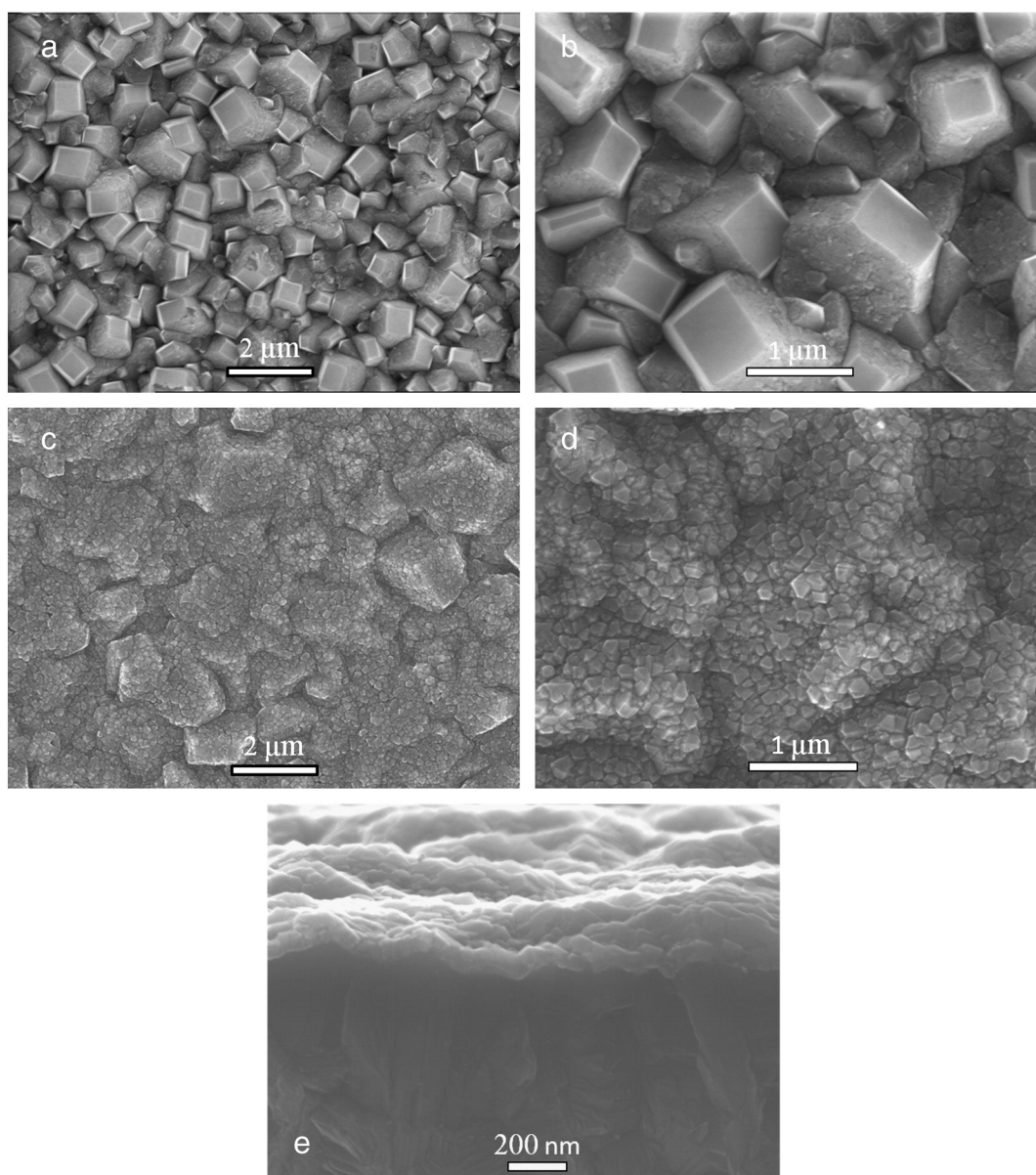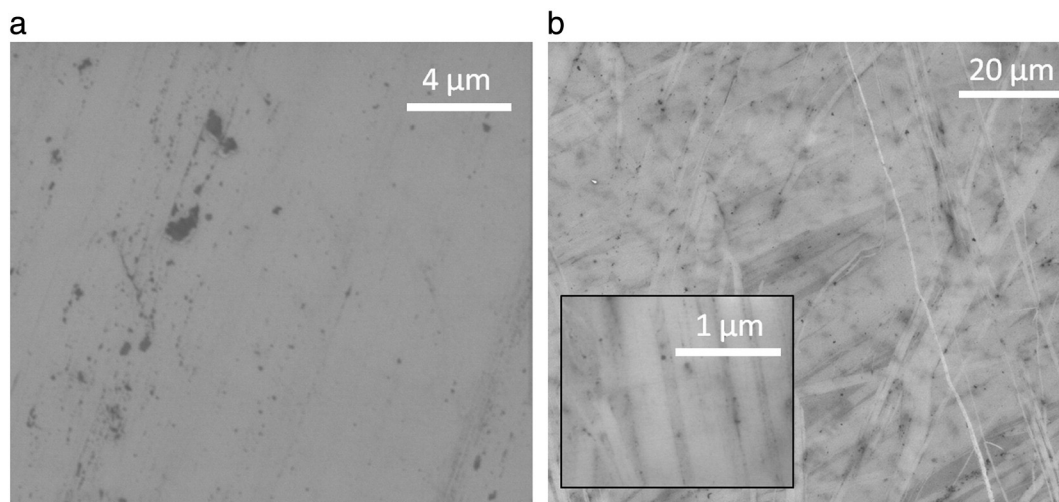

Fig. 2. SEM micrographs showing the morphologies of the two types of diamond films grown on Si substrates. (a) & (b) Nitrogen-doped microcrystalline diamond. (c), (d) & (e) Li–N-co-doped diamond with (e) showing a cross-section through the film.

Fig. 3. SEM micrographs of a HPHT substrate (a) before growth and (b) after growth of a 1-μm-thick nitrogen-doped diamond capping layer on top of a Li/N co-doped layer. The inset is at higher magnification. There are no obvious growth features on the surface, showing that the film was essentially homogeneous. The dark marks are believed to be artefacts of the SEM showing regions of lower secondary electron emission due to localised variation in H termination, and not due to changes in surface topology.

diamond growth process, with no visible defects or etch pits observed. Fig. 3(b) shows that after deposition of Li_3N followed by ~1 μm of N-doped diamond capping layer, the diamond surfaces did not show any signs of significant renucleation and/or new crystal formation — the new diamond layers appear to be homoepitaxial with the HPHT substrate. There are some new superficial discolorations visible on the surface, in the form of stripes and lines, but these are ≪1 μm in thickness and are probably due to variations in secondary electron emission yield from non-uniform H-termination. Raman spectra (not shown) show no sign of sp^2 carbon formed at new grain boundaries, indicating that the newly grown layers remain essentially single crystal. Similar surface effects were also observed on diamond films grown on the other HPHT substrates. These results are consistent with the idea mentioned above — because HPHT substrates are single crystal, there are no grain

boundaries to be etched by the Li, and so the film growth is more uniform with no secondary nucleation.

Fig. 4 shows the SIMS depth-profile analysis of a multilayered Li–N-co-doped diamond thin film. The carbon signal remains constant for all the layers and serves as the baseline from which to calculate the concentrations of Li and N. The Li signal is centred at a depth of ~200 nm beneath the diamond surface, with a spread of ~100 nm either side due to diffusion, with a possible contribution of ±10 nm due to SIMS mixing. The maximum concentration of Li detected was 5.0×10^{19} cm^{-3} with a total integrated dose of 3.7×10^{21} Li atoms throughout the diffusion region. The N signal was detected only in the first 500 nm inside the diamond thin film, as expected. The maximum concentration of nitrogen atoms embedded in the film was 4.4×10^{20} cm^{-3} which is ~9 times more than the Li content. This over-doping with N had been done to ensure all that all the Li atoms inside the diamond film were adjacent to at least one N and so were immobilised within the diamond lattice. It can be seen that the N-doped NCD that grew on the outer surface (topmost 50 nm) still contains a considerable amount of Li, and a reduction in N. This may due to the high solubility of Li in sp^2 carbon structures compared to diamond [40], which may have displaced some of the nitrogen.
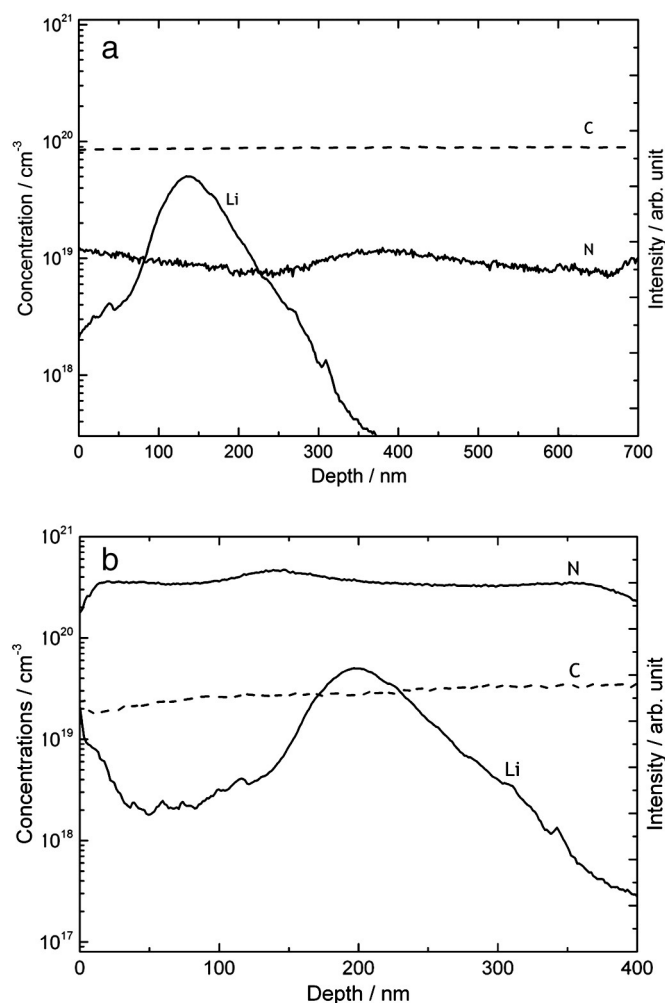
These results confirm that the Li_3N process followed by encapsulation produced a well-defined layer of diamond that contained localised high concentrations of N and Li. However, electrical testing showed that the 2-point resistivity of these films remained high (~15–50 MΩ) suggesting either that the Li or its associated LiN_x defect centre were electrically inactive.

3.2. Effect of changing precursors on Li and N incorporation

In order to test whether it was possible to control the amount of N and Li incorporation, two deposition experiments were performed where the same procedure (Si substrate, growth of 2 μm N-doped diamond, Li_3N drop cast, deposition of ~150–200 nm of N-doped capping layer) was performed using (i) N_2 as the source of nitrogen and 100 μl of Li_3N in the first experiment, and (ii) NH_3 and 200 μl of Li_3N in the second. The results are shown in Fig. 5(a) and (b). When using N_2 (Fig. 5(a)) the amount of N incorporation is $<1.1 \times 10^{19}$ cm^{-3} (below the SIMS detection limit) compared to the film deposited using NH_3 (Fig. 5(b)) with ~3.5×10^{20} cm^{-3}. Thus, nearly 10 times as much nitrogen is incorporated into the diamond when using NH_3 than when using N_2. This is because the energies available in a hot filament system are not sufficient to efficiently dissociate the strong triple bonds in N_2 (914 kJ mol^{-1}) compared to the weaker NH bonds (414 kJ mol^{-1}) in
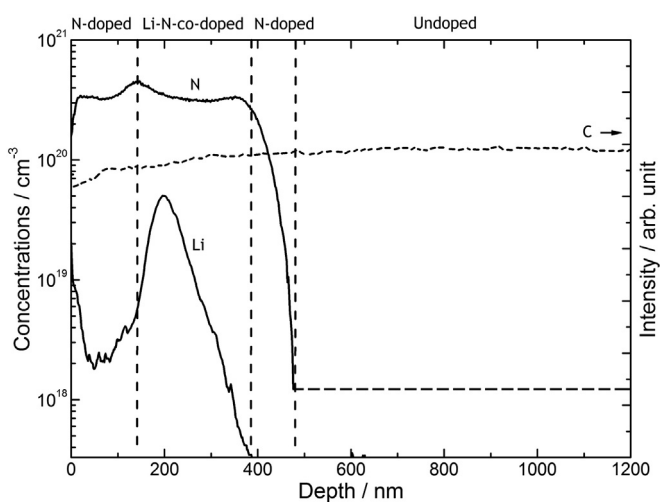
Fig. 4. SIMS depth profile of a multilayered Li–N-co-doped diamond film grown on a Si substrate. This film had the following layered structure, indicated by the dashed vertical lines, starting from the Si substrate: ~2 μm of undoped diamond, ~350 nm of nitrogen-doped diamond (grown using NH_3) of which the top ~250 nm has been transformed into a Li–N co-doped layer by diffusion into it of the Li_3N, ~150 nm N-doped diamond capping layer (which also shows some in-diffusion of Li in its lower 50 nm). Shown on the plot are the absolute calibrated concentrations of Li and N (left-hand axis), and C intensity (right-hand axis) which is used as the baseline from which the other concentrations were calculated, as a function of depth beneath the diamond surface. The dashed horizontal line for the N concentration shows the lower limit of detection when the mass 26 signal is due entirely to $C_2H_2^-$.

A fourth experiment was performed in which 2×100 μl of Li_3N was added to the diamond surface sequentially, with an hour bake in H_2 in between each addition. Again, subsequent diamond CVD resulted in the formation of the flaky lithium carbide. So we conclude that adding more Li to a diamond lattice that has reached its solid solution saturation point does not work, and the excess lithium reacts with the gas-phase carbon species to form lithium carbides, preventing further diamond deposition.

3.3. Multiple layers

In order to test whether it was possible to grow a diamond film with multiple embedded Li-rich layers, a sample was grown using the standard procedures outlined above, but with ammonia gas acting as the nitrogen precursor and repeated application of the Li_3N followed by an embedding layer. Fig. 6 shows the SIMS depth profile for a film that had the following deposition sequence: Si substrate, 1st addition of Li_3N to form 300 nm of Li–N co-doped diamond layer, 2nd addition of Li_3N to create 250 nm of Li–N co-doped diamond layer, 3rd addition of Li_3N to produce 80 nm of Li–N co-doped diamond layer, and finally 20 nm of capping layer consisting of undoped diamond. As expected, the Li atoms are present in three localised layers within the diamond film. The first two additions have the same peak Li concentration of ~1.0×10^{19} cm^{-3} while the final addition has concentration up to the proposed maximum limit of ~5.0×10^{19} cm^{-3}. The minimum amount of Li detected was ~1.0×10^{18} cm^{-3} while the concentration of N atoms inside the film during all three additions remained constant at ~1.8×10^{20} cm^{-3}. The concentration of the nitrogen dropped near the diamond surface due to the capping layer being grown without ammonia being present. This is essential to avoid any amine or other nitrogen derivatives terminating the diamond surface which may affect the conductivity of the film. However, the N:Li ratio was still 18:1, meaning that the dominant dopant of the film was nitrogen. Interestingly, the resistance of the film did not resemble the values obtained from typical nitrogen-doped diamond films (>200 MΩ at room temperature [3,14]), being 10–20 MΩ at room temperature. This suggests that the incorporation of lithium and nitrogen in this way may enhance the

Fig. 5. SIMS depth profiles (top 400 nm only) of samples grown with (a) N_2 gas and (b) NH_3 gas added to the CVD gas mixture. Li_3N was added after the film thickness was ~2 μm, and then a 200 nm capping layer was added using the same gas mixture as for the lower layer. The concentrations of Li and N are shown on the left-hand axis, while the C intensity is shown on the right-hand axis.

ammonia [41], although this difference would be less apparent in higher power microwave plasma systems.
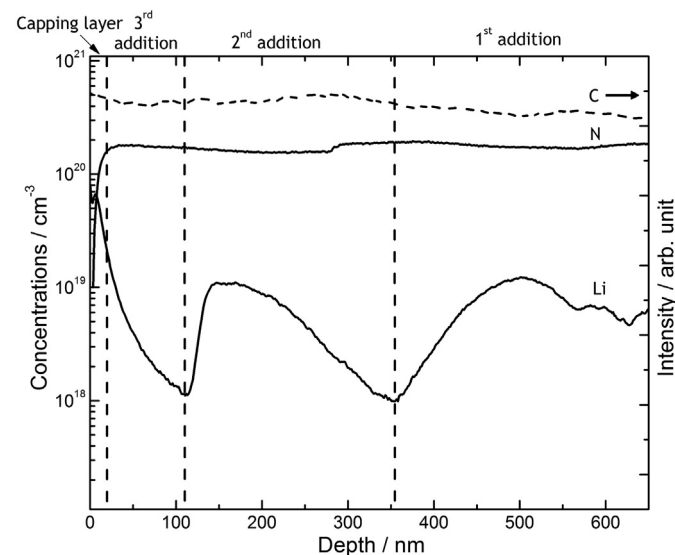
In contrast, doubling the amount of Li_3N had little effect upon either the maximum concentration of Li (5×10^{-19} cm^{-3}) or the total integrated amount of Li incorporated inside the films, which is ~4.0×10^{21} Li atoms in both cases. As before, the Li layer is localised ~200 nm below the surface, although diffusion has broadened the layer to a thickness ~300 nm. The diffusion profile is slightly asymmetric probably due to the longer diffusion time experienced by the Li atoms on the deeper side of the film. This suggests that it should be possible to fabricate multiple layers of localised Li-rich regions within the diamond.

The fact that doubling the Li_3N amount did not change the Li content inside the diamond film suggests that the amount of lithium has reached its solubility limit. To confirm this, a third sample was grown using the same conditions as (ii) above (i.e. using NH_3), but with an even higher amount of Li_3N (300 μl). When attempting to grow the capping layer, this instead produced a thin black flaky film which spontaneously delaminated upon opening the chamber. The black flakes were analysed using laser Raman spectroscopy and no diamond or graphite peaks were observed, while SIMS showed them to be composed of Li and C. These findings are consistent with the black flakes being a form of a lithium carbide (Li_2C_2, Li_4C, Li_6C_2, etc.), although no further analysis was performed to identify them more precisely.

Fig. 6. SIMS depth profile of a multi-layered Li–N co-doped diamond film grown on a Si substrate. This film had the following layered structure starting from the Si substrate: 1st layer of Li–N co-doped diamond, 2nd layer of Li–N co-doped diamond and then 3rd layer of Li–N co-doped diamond. The capping layer (~20 nm) was grown without the addition of ammonia into the gas phase. Shown on the plot are the absolute calibrated concentrations of Li and N (left-hand axis), and C intensity (right-hand axis), as a function of depth beneath the diamond surface.

conductivity of the film slightly but it is not yet sufficient for the film to be used in any semiconductor devices.

3.4. Single crystal HPHT substrate

To understand the role of grain boundaries in diffusion of lithium into diamond, the same procedures were repeated using single-crystal HPHT type Ib diamond. Two films were grown, the first using N_2 with 20 μl of Li_3N suspension and the other using NH_3 with 7 μl of Li_3N suspension, and with different thicknesses of capping layers. A larger amount of Li_3N suspension was used for the N_2 growth because of the expected difficulty of dissociation of N_2 gas. The growth procedure was: HPHT substrate, ~0.5 μm of N-doped diamond, Li_3N dropcast, N-doped capping layer (100 nm and 500 nm, respectively). Fig. 7 shows the SIMS depth profile for the two films. As before (see section (b)) there is ~10 times as much nitrogen present in the sample that was grown using NH_3 compared to the one grown using N_2. The total levels of N incorporated for both films are a factor of ~100 lower than for the microcrystalline diamond case; indeed, for the N_2-grown sample the N content throughout the bulk of the film is below the detection limits except within the Li_3N layer. For Li it is interesting to compare the width of the Li peaks to gain insight into Li diffusion. For the microcrystalline films the Li peak had a spread of about 200 nm either side of the centre, whereas for single-crystal diamond the spread is much less (± 50 nm for the NH_3-grown sample) for the equivalent deposition time, of which ± 10 nm may be attributed to SIMS mixing. These findings suggest that grain boundaries play an important role in helping both N and Li diffuse through diamond, and they may even trap many of these species within the sp^2 grain boundaries.

Two-point probe measurements showed that the resistance of these films remained at values similar to those found from the pure HPHT substrate alone (>1 MΩ over 3 mm probe separation), again suggesting that the dopants were not present in form that can significantly change the material conductivity. As before, with such high resistance values it was decided that more detailed electrical characterization (such as Hall effect measurements) would not be worthwhile.

4. Conclusions

Successful doping of diamond involves solving two problems (a) how to incorporate a high enough concentration of suitable dopants without damaging the diamond structure, and (b) how to make the dopants electrically active. The solution to (b) will need more work, of course, but at least researchers now have a new way to attack the
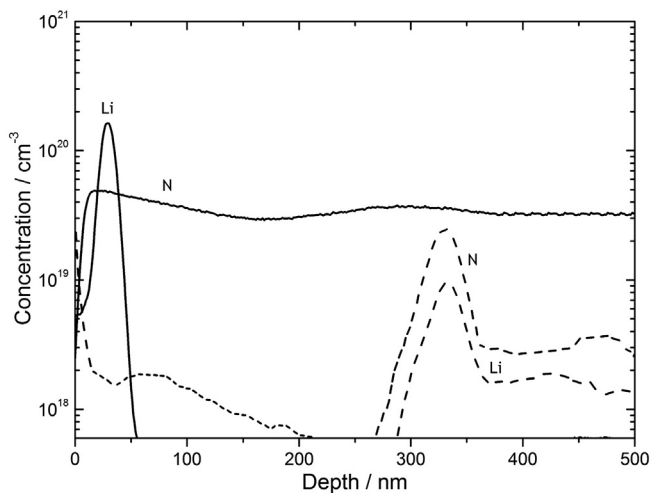
problem. We have demonstrated that it is possible to incorporate high concentrations of both dopants (Li, N) into different types of diamond films using solid Li_3N and gaseous NH_3 as sources of Li and N, respectively. The concentrations of both these species are as high, or even higher, than those reported by other methods, such as in-diffusion or implantation, while not suffering from the lattice damage or poor process control that these other methods sometimes involve, and thus may be one viable solution to problem (a).

However, it appears that there is a solid solubility limit of around 5×10^{19} cm^{-3} for Li in diamond, above which the Li no longer incorporates but instead reacts with the gas-phase CVD species to form carbides. Below this limit, the Li content can be controlled and localised into well-defined layers with a spread of ± 200 nm for microcrystalline diamond and ± 50 nm for single-crystal diamond. This difference in diffusion between the two types of diamond has been attributed to the presence of grain boundaries which we suggest aid diffusion of both Li and N throughout the bulk. The fact that these species can be incorporated at concentrations 10–100 times higher in MCD than in SCD films also suggests that the grain boundaries act as sinks for these species. Thus, Li and N in grain boundaries may be mobile along and within the grain boundary network, but do not migrate into the grains themselves where the diffusion is much slower. This model helps explain why the electrical conductivity of the Li/N-doped films remained so low, despite the dopant concentrations being so high. Perhaps much of the Li and N is trapped as electrically inactive species within the sp^2 grain boundaries. Alternatively, it may be that the optimal ratio of Li:N was not obtained in these preliminary experiments, and a more exhaustive series of experiments needs to be performed with a wider range of Li:N ratios. Computer modelling of Li and N within the diamond lattice is currently being performed [42] to help identify the optimal ratio that might give electrically active n-type diamond. Thus, although the dropcast method described in this paper appears to be a viable method to incorporate other potential n-type dopants, such as Mg, Na, etc., problem (b), making these dopants electrically active, remains as a challenge for future research.

Prime novelty statement

This paper demonstrates for the first time that large amounts of lithium and nitrogen can be incorporated simultaneously into a thin diamond film during the CVD growth process. It describes in detail how these potential dopants can be positioned in well-defined layers within the diamond film.

Fig. 7. SIMS depth profiles (top 500 nm only) of two Li–N co-doped diamond films grown on HPHT type Ib substrates using NH_3 (solid lines) or N_2 (dashed lines) as the nitrogen precursors.

References

[1] R. Kalish, Doping of diamond, Carbon 37 (1999) 781–785.
[2] P.W. May, M. Davey, K.N. Rosser, P.J. Heard, Arsenic and antimony doping: an attempt to deposit n-type CVD diamond, Mater. Res. Soc. Symp. Proc. 1039 (2007) (1039-P1015-1001).
[3] V. Baranauskas, B.B. Li, A. Peterlevitz, M.C. Tosin, S.F. Durrant, Nitrogen-doped diamond films, J. Appl. Phys. 85 (1999) 7455–7458.
[4] S. Koizumi, T. Teraji, H. Kanda, Phosphorus doped CVD diamond, Diamond Relat. Mater. 9 (2000) 935–940.
[5] J.R. Petherbridge, P.W. May, G.M. Fuge, G.F. Robertson, K.N. Rosser, M.N.R. Ashfold, Sulfur doping of diamond films: spectroscopic, electronic and gas-phase studies, J. Appl. Phys. 91 (2002) 3605–3613.
[6] K. Haenen, K. Meykens, M. Nesládek, G. Knuyt, L.M. Stals, T. Teraji, S. Koizumi, E. Gheeraert, Electronic states of phosphorus in diamond, Diamond Relat. Mater. 9 (2000) 952–955.
[7] M. Nesládek, K. Meykens, K. Haenen, L.M. Stals, T. Teraji, S. Koizumi, Low-temperature spectroscopic study of n-type diamond, Phys. Rev. B 59 (1999) 14852–14855.

[8] K. Haenen, A. Lazea, J. Barjon, J. D'Haen, N. Habka, T. Teraji, S. Koizumi, V. Mortet, P-doped diamond grown on (110)-textured microcrystalline diamond: growth, characterization and devices, J. Phys. Condens. Matter 21 (2009) 364204.

[9] F.A.M. Koeck, R.J. Nemanich, A. Lazea, K. Haenen, Thermionic electron emission from low work-function phosphorus doped diamond films, Diamond Relat. Mater. 18 (2009) 789–791.

[10] M.-A. Pinault-Thaury, B. Berini, I. Stenger, E. Chikoidze, A. Lusson, F. Jomard, J. Chevallier, J. Barjon, High fraction of substitutional phosphorus in a (100) diamond epilayer with low surface roughness, Appl. Phys. Lett. 100 (2012) 192109.

[11] S. Koizumi, M. Kamo, Y. Sato, S. Mita, A. Sawabe, A. Reznik, C. Uzan-Saguy, R. Kalish, Growth and characterization of phosphorus doped n-type diamond thin films, Diamond Relat. Mater. 7 (1998) 540–544.

[12] S. Jin, T.D. Moustakas, Effect of nitrogen on the growth of diamond films, Appl. Phys. Lett. 65 (1994) 403–405.

[13] A.J. Eccles, T.A. Steele, A. Afzal, C.A. Rego, W. Ahmed, P.W. May, S.M. Leeds, Influence of B- and N-doping levels on the quality and morphology of CVD diamond, Thin Solid Films 343–344 (1999) 627–631.

[14] J. Mort, M.A. Machonkin, K. Okumura, Compensation effects in nitrogen-doped diamond thin films, Appl. Phys. Lett. 59 (1991) 3148–3150.

[15] A. Badzian, T. Badzian, S.T. Lee, Synthesis of diamond from methane and nitrogen mixture, Appl. Phys. Lett. 62 (1993) 3432–3434.

[16] R. Locher, C. Wild, N. Herres, D. Behr, P. Koidl, Nitrogen stabilized 100 texture in chemical vapor deposited diamond films, Appl. Phys. Lett. 65 (1994) 34–36.

[17] W. Muller-Sebert, E. Worner, F. Fuchs, C. Wild, P. Koidl, Nitrogen induced increase of growth rate in chemical vapor deposition of diamond, Appl. Phys. Lett. 68 (1996) 759–760.

[18] K.M. O'Donnell, T.L. Martin, N.A. Fox, D. Cherns, The Li-adsorbed C(100)–(1 × 1):O diamond surface, Mater. Res. Soc. Symp. Proc. 1282 (2011).

[19] K.M. O'Donnell, T.L. Martin, N.A. Fox, D. Cherns, *Ab initio* investigation of lithium on the diamond C(100) surface, Phys. Rev. B 82 (2010) 115303.

[20] K.M. O'Donnell, M.T. Edmonds, J. Ristein, A. Tadich, L. Thomsen, Q.-H. Wu, C.I. Pakes, L. Ley, Diamond surfaces with air-stable negative electron affinity and giant electron yield enhancement, Adv. Func. Mater. 23 (2013) 5608–5614.

[21] J.P. Goss, R.J. Eyre, P.R. Briddon, Theoretical models for doping diamond for semiconductor applications, Phys. Status Solidi B 245 (2008) 1679–1700.

[22] E.B. Lombardi, A. Mainwood, A first principles study of lithium, sodium and aluminum in diamond, Diamond Relat. Mater. 17 (2008) 1349–1352.

[23] G. Popovici, M.A. Prelas, T. Sung, S. Khasawinah, A.A. Melnikov, V.S. Varichenko, A.V. Denisenko, W.R. Fahrner, Properties of diffused diamond films with n-type conductivity, Diamond Relat. Mater. 4 (1995) 877–881.

[24] M. Restle, K. Bharuth-Ram, H. Quintel, C. Ronning, H. Hoffsäss, S.G. Jahn, U. Wahl, Lattice sites of ion implanted Li in diamond, Appl. Phys. Lett. 66 (1995) 2733–2735.

[25] S. Prawer, C. Uzan-Saguy, G. Braunstein, R. Kalish, Can n-type doping of diamond be achieved by Li or Na ion implantation? Appl. Phys. Lett. 63 (1993) 2502–2504.

[26] R. Job, M. Werner, A. Denisenko, A. Zaitsev, W.R. Fahrner, Electrical properties of lithium-implanted layers on synthetic diamond, Diamond Relat. Mater. 5 (1996) 757–760.

[27] I.M. Buckley-Golder, R. Bullough, M.R. Hayns, J.R. Willis, R.C. Piller, N.G. Blamires, G. Gard, J. Stephen, Post-processing of diamond and diamond films: a review of some Harwell work, Diamond Relat. Mater. 1 (1991) 43–50.

[28] C. Cytermann, R. Brener, R. Kalish, Search for diffusion of Li implants in natural and polycrystalline CVD diamond, Diamond Relat. Mater. 3 (1994) 677–680.

[29] G. Popovici, T. Sung, S. Khasawinah, M.A. Prelas, Forced diffusion of impurities in natural diamond and polycrystalline diamond films, J. Appl. Phys. 77 (1995) 5625–5629.

[30] C. Uzan-Saguy, C. Cytermann, B. Fizgeer, V. Richter, R. Brener, R. Kalish, Diffusion of lithium in diamond, Phys. Status Solidi A 193 (2002) 508–516.

[31] G.G. Fountain, R.A. Rudder, D.P. Malta, S.V. Hattangady, R.G. Alley, G.C. Hudson, J.B. Potshill, R.J. Markunas, T.P. Humphreys, R.J. Nemanich, V. Venkatesan, K. Das, IGFET fabrication on homoepitaxial diamond using in situ boron and lithium doping, Diamond Mater Proc. 2nd Symp. Electrochem. Soc., 91–8, 1991, pp. 523–529.

[32] K. Okumura, J. Mort, M. Machonkin, Lithium doping and photoemission of diamond thin films, Appl. Phys. Lett. 57 (1990) 1907–1909.

[33] R. Zeisel, C.E. Nebel, M. Stutzmann, H. Sternschulte, M. Schreck, B. Stritzker, Photoconductivity study of Li doped homoepitaxially grown CVD diamond, Phys. Status Solidi A 181 (2000) 45–50.

[34] A. Namba, Y. Yamamoto, H. Sumiya, Y. Nishibayashi, T. Imai, Process for producing n-type semiconductor diamond and n-type semiconductor diamond, United States Pat., US 0177962 A1 (2006).

[35] A. Namba, T. Imai, H. Takeuchi, Low resistivity N-type semiconductor diamond and method of its manufacture, United States Pat., US 7255744 B2 (2007).

[36] J.E. Moussa, N. Marom, N. Sai, J.R. Chelikowsky, Theoretical design of a shallow donor in diamond by lithium–nitrogen codoping, Phys. Rev. Lett. 108 (2012) 226404.

[37] P.W. May, P.R. Burridge, C.A. Rego, R.S. Tsang, M.N.R. Ashfold, K.N. Rosser, R.E. Tanner, D. Cherns, R. Vincent, Investigation of the addition of nitrogen-containing gases to a hot filament diamond CVD reactor, Diamond Relat. Mater. 5 (1996) 354–358.

[38] R.S. Tsang, C.A. Rego, P.W. May, M.N.R. Ashfold, K.N. Rosser, Diamond Relat. Mater. 6 (1997) 247.

[39] H. Sachdev, Comparative aspects of the homogeneous degradation of c-BN and diamond, Diamond Relat. Mater. 10 (2001) 1390–1397.

[40] N.A. Kaskhedikar, J. Maier, Lithium storage in carbon nanostructures, Adv. Mater. 21 (2009) 2664–2680.

[41] J.A. Smith, J.B. Wills, H.S. Moores, A.J. Orr-Ewing, M.N.R. Ashfold, Y.A. Mankelevich, N.V. Suetin, Effects of NH_3 and N_2 additions to hot filament activated CH_4/H_2 gas mixtures, J. Appl. Phys. 92 (2002) 672–681.

[42] M. Z. Othman, J. N. Hart, K. M. O'Donnell, P. W. May, N. L. Allan, (2014), in preparation.